A

Au/CuO$_x$−TiO$_2$ Catalysts for Preferential Oxidation of CO in Hydrogen Stream

Palanivelu Sangeetha, Bin Zhao, and Yu-Wen Chen*

Department of Chemical Engineering, National Central University, Chung-Li 320, Taiwan

A series of Au/CuO$_x$−TiO$_2$ catalysts with various Cu/Ti atomic ratios were prepared by deposition−precipitation method. The catalysts were characterized by inductively coupled plasma−mass spectrometry, X-ray diffraction, transmission electron microscopy, high-resolution transmission electron microscopy, and X-ray photoelectron spectroscopy. The preferential oxidation of CO in H$_2$ stream (PROX) on these catalysts was carried out in a fixed bed microreactor with a gas mixture (CO:O$_2$:H$_2$:He = 1.33:1.33:65.33:32.01 by volume ratios) was fed with a space velocity of 30000 mL/(g·h). Au/CuO$_x$−TiO$_2$ with various Cu/Ti atomic ratios showed similar gold particle size (2.3−2.5 nm). The gold in the starting material was almost totally loaded on the CuO$_x$−TiO$_2$ support at pH = 7. Au/CuO$_x$−TiO$_2$ catalysts with gold content of 1 wt % and calcined at 180 °C had superior catalytic activity and selectivity for CO oxidation at temperature of 80 °C. Au/CuO$_x$−TiO$_2$ (Cu/Ti = 4.8/95.2) had a CO conversion of 100% at 80 °C, and CO selectivity reaches 68%. Gold particles were well dispersed and stable on the support. Even after PROX reaction at 80 °C for a long time, most of the particles still maintained at ∼2.4 nm. The CO conversion slightly decreased from 100% to 95%, and CO selectivity was nearly the same. Au/CuO$_x$−TiO$_2$ is a highly effective and thermally stable catalyst for PROX reaction compared with Au/TiO$_2$ catalyst.

1. Introduction

Gold was regarded as a catalytically inactive material for a long time because of its deep lying valence d band and very diffuse valence s and p orbitals.[1] This situation has been changed in recent years with the discovery of the catalytic activity of gold nanoparticles.[2] Gold catalysts have recently gained attention due to their potential for many reactions of both industrial and environmental importance. The most studied catalyst for preferential oxidation of CO in H$_2$ stream is gold supported on TiO$_2$ because it is one of the most active catalysts for this reaction at low temperature. The optimum gold particle size in these catalysts was found to be ∼3 nm. Studies on gold catalysts so far showed that the macroscopic gold is only weakly active for CO oxidation; Au in nanodispersed form, with strong metal−support interaction, leads to highly active catalysts.[3,4] Several techniques, such as coprecipitation,[5] deposition−precipitation,[6] chemical vapor deposition,[7] impregnation,[8] and photodeposition method[9] have been used for the synthesis of nanogold particles on metal oxides.

The activity of gold catalyst depends on the nature of support, particle size of gold, and preparation method. Deposition−precipitation (DP) method has been extensively used to prepare gold catalyst supported on several metal oxides.[6] Transition metals supported on some oxides are good substitute catalysts because of their low-price and widespread use. Among them, copper or copper oxide can exhibit activities per unit surface area to those of noble metal catalysts such as platinum in CO oxidation. Copper or copper oxides supported on TiO$_2$ are active in catalyzing selective CO oxidation in the presence of O$_2$. Friedman and Freeman[10] pointed out that beyond a critical quantity, any additional copper loading was in the form of bulk crystalline oxide. Liu and Flytzani-stephanopoulos[11] suggested that the activity of catalyst derived primarily from the combination of finely dispersed copper-support systems, and bulk copper oxide had negligible contributions. Similar results reported by Yu et al.[12] indicated that the best catalytic effect is achieved when the amount of CuO$_x$ is near the monolayer dispersion threshold, a higher amount of CuO$_x$ loading would have reverse effect. Shihua Wu et al.[13] reported that CuO$_x$−TiO$_2$ could oxidize CO completely above 100 °C. They suggested that the CuO$_x$−TiO$_2$ catalyst is an active and stable catalyst for CO oxidation. The TiO$_2$ particles acted as the support and the CuO$_x$ acted as an active component above 100 °C.

DP method has been regarded as the most simple and cost-effective method to prepare gold catalysts. Liu and Vannice[14] have reported that the deposition of Au on the surface of TiO$_2$ markedly enhances the catalytic activity for CO oxidation. Our earlier study focused on several catalyst systems such as Au/MnO$_x$−TiO$_2$[15] and Au/MgO$_x$−TiO$_2$[16] catalysts for preferential oxidation of CO in H$_2$ stream. These materials were more selective for CO oxidation in H$_2$ stream.[15−22] Au/CuO−TiO$_2$ has not been studied for PROX reaction. Since CuO is also active for CO oxidation, it would be interesting to investigate if adding CuO could improve the activity and selectivity in PROX reaction.

The objective of the present study was to investigate the CuO-promoted Au/TiO$_2$ catalyst for preferential oxidation of CO in a H$_2$ stream (PROX). The effect of content of CuO was investigated. The catalysts were characterized by XRD, TEM, and XPS.

2. Experimental Section

2.1. Preparation of CuO$_x$−TiO$_2$ Support. CuO$_x$−TiO$_2$ supports with different molar ratios (Cu/Ti = 1/99, 2/98, 4.7/95.3, and 10/90) were prepared by incipient-wetness impregnation. Suitable amount of Cu(NO$_3$)$_3$·3H$_2$O (Merck) were dissolved in distilled water according to the weight of TiO$_2$ (Degussa P25) powder. Copper nitrate solution was added to TiO$_2$ powder slowly by dropwise with continuous stirring. The sample was dried at 100 °C and then calcined at 350 °C for 4 h. The sample was ground to fine powder.

2.2. Preparation of Au/CuO$_x$−TiO$_2$. Gold catalysts were prepared by deposition−precipitation method. HAuCl$_4$ (Aldrich) solution was poured at a rate 10 mL/min into an aqueous

* To whom correspondence should be addressed. E-mail: ywchen@cc.ncu.edu.tw. Tel.: 886 34227151 ext. 34203. Fax: 886 34252296.

Table 1. ICP−MS Analysis for Au and Cu Content and Average Au Particle Size (Cu/Ti by Atom Ratio)

catalyst	actual Au loading (wt %)	actual Cu loading (wt %)	average Au particle size (nm)
1% Au/CuO$_x$−TiO$_2$ (1:99)	0.976	0.825	2.39
1% Au/CuO$_x$−TiO$_2$ (2:98)	0.952	1.417	2.41
1% Au/CuO$_x$−TiO$_2$ (4.8:95.2)	0.931	3.135	2.45
1% Au/CuO$_x$−TiO$_2$ (10:90)	0.832	7.926	2.57

solution of CuO$_x$−TiO$_2$ support under vigorous stirring. The temperature of solution was maintained at 65 °C, and 1 N NH$_4$OH solution was used to adjust pH to 7. After aging for 2 h, the precipitate was filtered and washed with hot water (65 °C) until no Cl$^−$ was detected with AgNO$_3$ solution. It was then dried at 80 °C for 12 h. Finally, the cake was ground and then calcined at 180 °C for 4 h and ground again to obtain gold catalysts.

2.3. Characterization. The catalysts were characterized by inductively coupled plasma−mass spectrometry (ICP−MS), powder X-ray diffraction (XRD), transmission electron microscopy (TEM), and X-ray photoelectron spectroscopy (XPS).

The gold content of the as-prepared catalyst was determined by ICP−MS (PE-SCIEX ELAN 6100 DRC). The catalyst was digested with a mixture of 1 mL of HNO$_3$ (65%), 3 mL of HCl (37%) and 5 mL of HF (40%) in a microwave oven. ICP−MS was connected to a Geolas Excimer laser ablation system, which features a homogenized 193 nm ArF laser beam and output energy of 30 mJ/cm^2.

XRD was performed using a Siemens D500 powder diffractometer. The XRD patterns were collected using CuKα$_1$ radiation (λ = 0.15405 nm) at a voltage and current of 40 kV and 40 mA, respectively. The sample was scanned over the range 2θ = 20−70° at a rate of 0.05° s^{-1} to identify the crystalline structure. The sample for XRD was prepared as a thin layer on a sample holder.

The morphology and particle size of the samples were determined by TEM on a JEM-2000 FX II operated at 200 kV. Initially, a small amount of sample was loaded into the sample bottle filled with absolute methanol solution. A drop of the dispersed slurry was dropped onto a carbon-coated copper grid (300#) (Ted Pella Inc., CA, USA), and after agitating under ultrasonic environment for 30 min it was dried in an oven at 80 °C for 10 h.

The XPS spectra were recorded on a Thermo VG Scientific Sigma Probe spectrometer using Al Kα radiation as the exicitation source (hν = 1486.6 eV) (20 kV, 30 mA). The
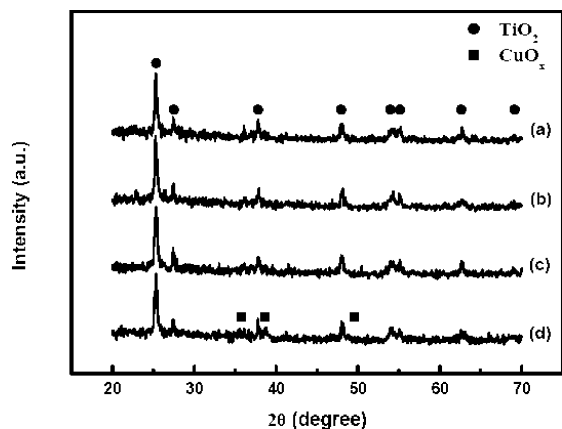

(a) 1 wt.% Au/CuO$_x$-TiO$_2$ (1:99)   (b) 1 wt.% Au/CuO$_x$-TiO$_2$ (2:98)

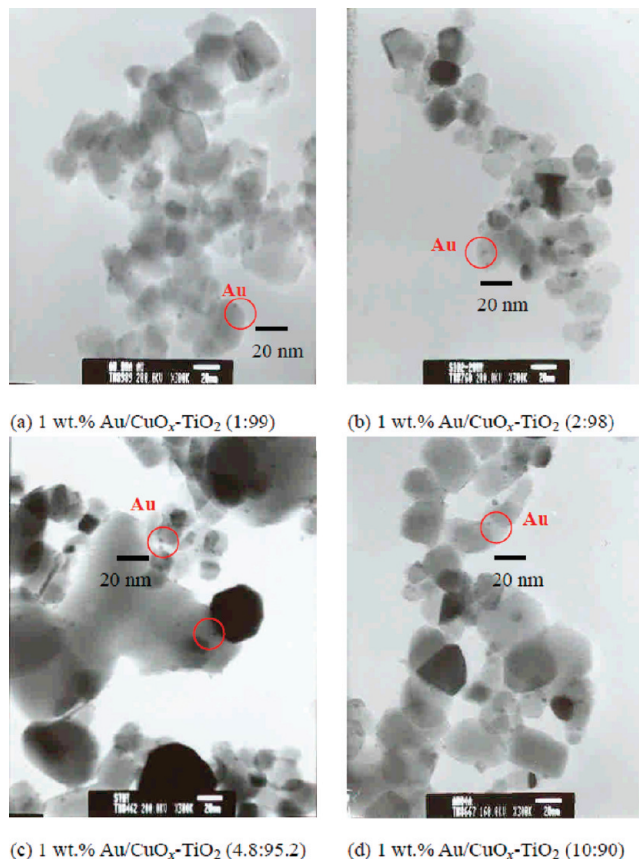(c) 1 wt.% Au/CuO$_x$-TiO$_2$ (4.8:95.2)   (d) 1 wt.% Au/CuO$_x$-TiO$_2$ (10:90)

Figure 2. TEM photos of Au/CuO$_x$−TiO$_2$ catalysts.

sample pressed into a self-supported disk was mounted on the sample plate. Then it was degassed in the pretreatment chamber at 343 K for 2 h in vacuo before being transferred into the analyzing chamber where the background pressure was lower than 2×10^{-9} Torr. The binding energy of each element was corrected using the C1s level of contaminant carbon (binding energy = 284.5 eV). Before the XPS analysis, the sample was pretreated by Ar$^+$ sputtering for 5 min to remove the oxidized layer. The XPS peaks were decomposed into subcomponents using a Gaussian−Lorentzian curve-fitting program. The surface composition of each catalyst was calculated using the corresponding peak areas of Au and Cu; the PHI sensitivity factors for these elements were multiplied to the peak areas.

2.2. Catalytic Reaction. The catalytic activity of PROX reaction on gold catalyst was measured in a downward, fixed-bed, continuous-flow reactor made of Pyrex glass. The catalyst (0.1 g) was pretreated by reactant gas for 1 h. The reactant gas containing 1.33% CO, 1.33% O$_2$, 65.33% H$_2$, and 32.01% He for balance (vol. %) was passed into the reactor with a flow rate of 50 cc/min (GHSV = 30000 mL/(h·g) catalyst). O$_2$/CO molar ratio was 1 in the feed gas. Limited O$_2$ was used to differentiate the activities and selectivities of the catalysts in this study. The reactor was heated by a regulated furnace (heating rate = 1 °C/min), and the temperature was measured by a thermocouple placed inside the catalyst bed. Several criteria were used to confirm that the reaction was operated in the absence of heat and mass transfer effects. The outlet gas was analyzed by an on-line gas chromatography equipped with a thermal conductivity detector. The product sample was separated by a MS-5A column. Calibration was done with a standard gas containing known concentrations of the com-
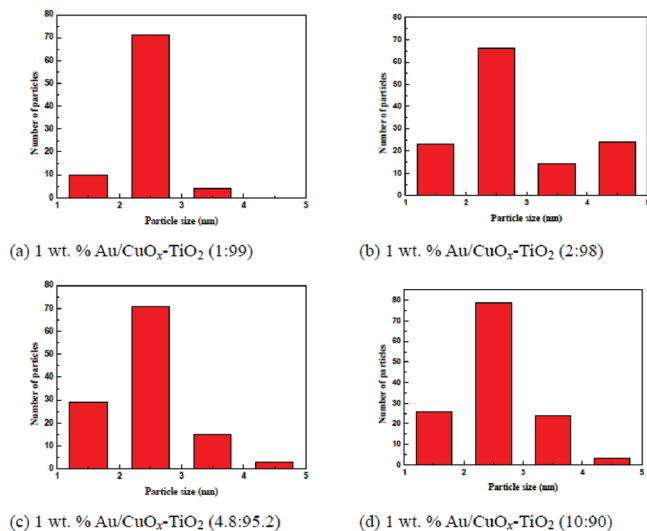

Figure 1. XRD patterns of (a) 1 wt % Au/CuO$_x$−TiO$_2$ (1:99); (b) 1 wt % Au/CuO$_x$−TiO$_2$ (2: 98); (c) 1 wt % Au/CuO$_x$−TiO$_2$ (4.8: 95.2); (d) 1 wt % Au/CuO$_x$−TiO$_2$ (10: 90).

Figure 3. Distribution of gold particle size and the number average diameter.

Figure 5. Cu 2p XPS spectra of (a) 1 wt % Au/CuO$_x$−TiO$_2$ (1:99); (b) 1 wt % Au/CuO$_x$−TiO$_2$ (2:98); (c) 1 wt % Au/CuO$_x$−TiO$_2$ (4.8:95.2); (d) 1 wt % Au/CuO$_x$−TiO$_2$ (10:90).

ponents. The CO conversion (X_{CO} %), O$_2$ conversion (X_{O_2} %) and selectivity of O$_2$ reacting with CO (S %) were calculated as follows:

$$\text{CO conversion } (X_{CO} \%) = \frac{[CO]_{in} - [CO]_{out}}{[CO]_{in}} \times 100\%$$

(1)

$$\text{O}_2 \text{ conversion } (X_{O_2} \%) = \frac{[O_2]_{in} - [O_2]_{out}}{[O_2]_{in}} \times 100\% \quad (2)$$

CO selectivity is the percentage of O$_2$ reacting with CO. The definition of CO selectivity is

$$\text{selectivity of O}_2 \text{ reacting with CO } (S\%) = \frac{0.5 X_{CO}}{X_{O_2}} \times 100\%$$

(3)

= mol of O$_2$ reacting with CO/mol of O$_2$ consumed.

3. Results and Discussion

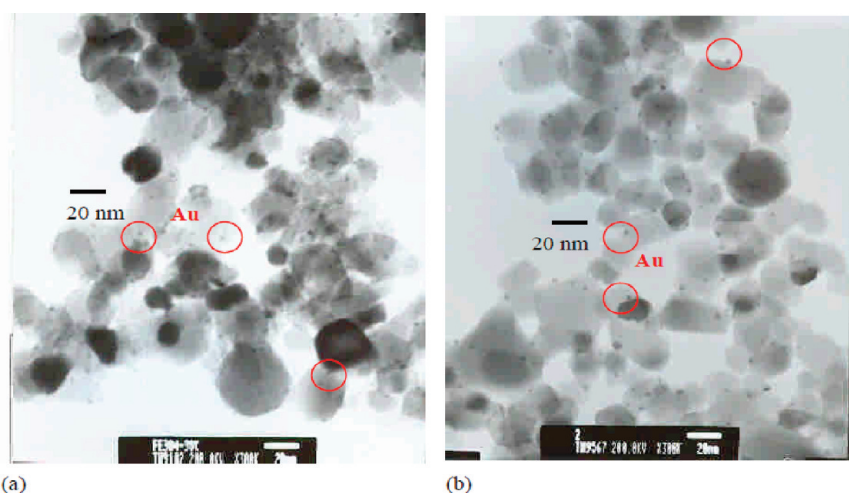**3.1. ICP−MS.** ICP-MS results are listed in Table 1. Gold was loaded nearly 100% by deposition−precipitation method on CuO$_x$−TiO$_2$ support. The real gold contents of Au/CuO$_x$−CeO$_2$−TiO$_2$ (4.8:9.6:85.6) and Au/CuO$_x$−TiO$_2$ (4.8:95.2) were close. Au/CuO$_x$−TiO$_2$ (10:90) had the lowest gold content of 0.832 wt %. It is known that only about half of gold in the starting material could be deposited on TiO$_2$.[2,3] The results demonstrated that the presence of CuO could influence the surface properties of TiO$_2$ thereby resulting in higher gold deposition on CuO−TiO$_2$ support.

3.2. XRD. The XRD patterns of Au/CuO$_x$−TiO$_2$ catalysts with various Cu/Ti ratios are shown in Figure 1. The diffraction peaks of TiO$_2$ appeared at $2\theta = 25.23°$ (101), 37.72° (004), 47.89° (200), 53.77° (105), and 62.51° (204) for TiO$_2$ at anatase state, $2\theta = 27.45°$ (110), 36.10° (101), and 54.36° (211) were ascribed to rutile phase. The peak intensities gradually decreased with increasing Cu/Ti ratio, as expected due to the decrease of TiO$_2$ content. The preparation and pretreatment did not change the crystalline phase of P25 TiO$_2$. A progressive enhancement of the crystallite size of CuO was identified, as reflected from a continuous sharpening and intensification of the diffraction peaks for the catalysts with increasing Cu/Ti ratios.

As shown in Figure 1, only weak and broad diffraction peaks of CuO were observed for the support calcined at 350 °C,

Figure 4. TEM photos of 1% Au/CuO$_x$−TiO$_2$ (4.8:95.2) for lifetime test: (a) PROX at 80 °C for 49 h; (b) after storage the 1 wt % Au/CuO$_x$−TiO$_2$ (4.8:95.2) catalyst for one month.
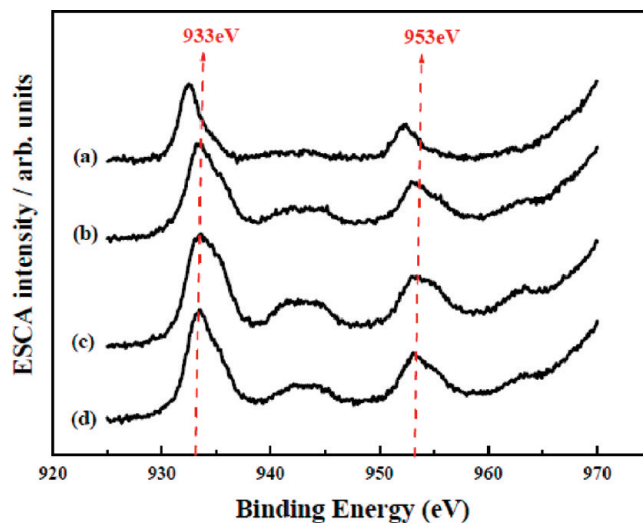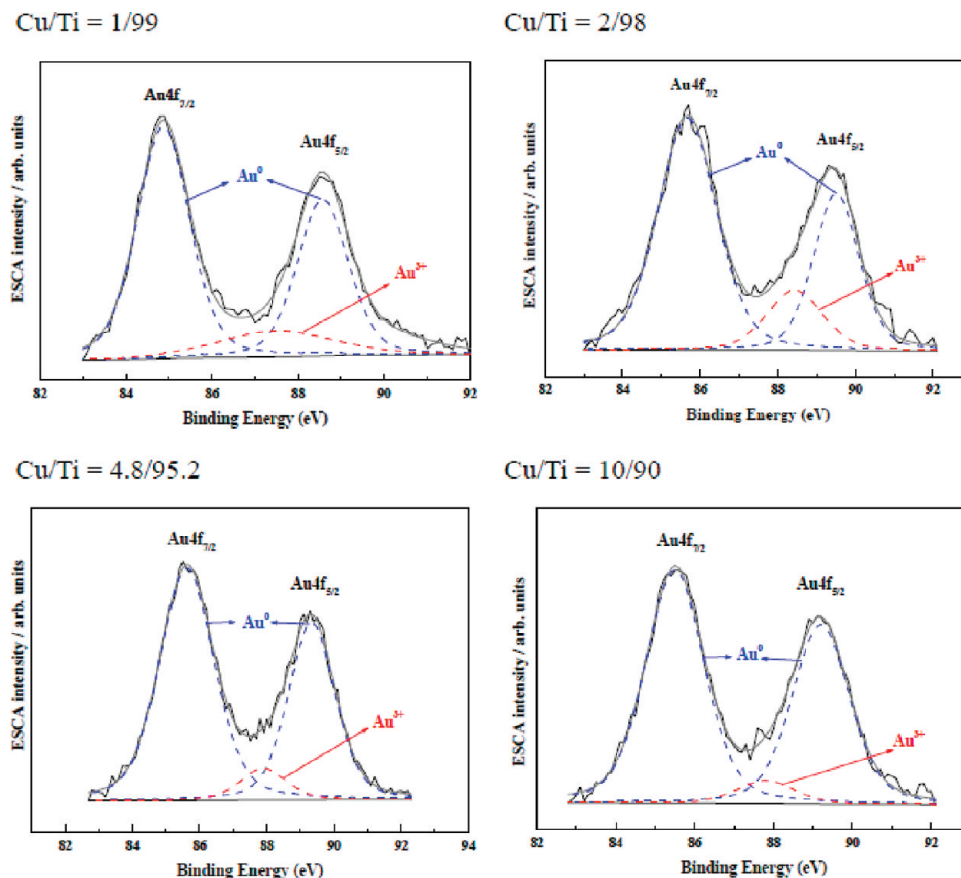
Figure 6. Effect of Cu/Ti mole ratios overAu/CuO$_x$−TiO$_2$ catalysts for XPS patterns of (a) 1 wt % Au/CuO$_x$−TiO$_2$ (1:99); (b) 1 wt % Au/CuO$_x$−TiO$_2$ (2:98); (c) 1 wt % Au/CuO$_x$−TiO$_2$ (4.8:95.2); (d) 1 wt % Au/CuO$_x$−TiO$_2$ (10:90).

pointing to an amorphous and well-dispersed CuO on TiO$_2$ surface. In Figure 1a−d, the diffraction peaks of CuO in Au/CuO$_x$−TiO$_2$ catalysts were weak, probably due to the formation of thin CuO surface layer on TiO$_2$. By comparing the XRD patterns, the results confirmed that the crystalline form of copper oxide was CuO on the TiO$_2$ catalyst. The calculated average CuO crystallite size by using Scherrer's equation was 15−20 nm. It was noted that there was no peak corresponding to gold species. It is because that the gold particles were too small to be detected. Even with a reaction at 80 °C for a long time, the Au particle was still stable, since no XRD peaks for Au species were observed. The results are in agreement with that of Bandara et al.[23] They reported that it was due to the presence of noticeable amorphous CuO.

3.3. TEM. To identify the gold particle size, TEM images were used to calculate the number average particle size. Gold particles are visible as black dots in the TEM images and homogeneously dispersed on the surface of CuO$_x$−TiO$_2$ and TiO$_2$ support, respectively. The black bulk portion of about 20 nm is CuO$_x$ and light gray region is TiO$_2$. Figure 2 shows the TEM images of the Au/CuO$_x$−TiO$_2$ catalysts with various Cu/Ti molar ratios. Figure 3 shows the particle size distribution of Au catalysts. The mean particle diameter of gold for Au/CuO$_x$−TiO$_2$ was about 2.39−2.57 nm. When the loading of CuO$_x$ was increased, a slight increase in gold particle size was observed. It means that gold was highly dispersed and formed small particles. Figure 4 shows that the 1 wt % Au/CuO$_x$−TiO$_2$ (4.8:95.2) still had the small gold particle after 49 h time on stream in PROX reaction at 80 °C. It is obvious that a small amount of 4−5 nm gold particles appeared after reaction, but
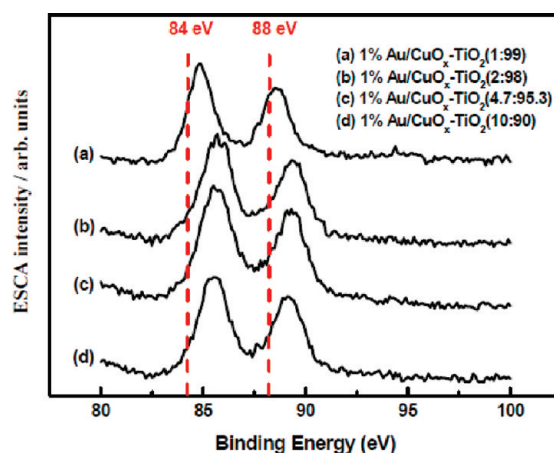

Figure 7. Comparative Au 4f XPS patterns of (a) 1 wt % Au/CuO$_x$−TiO$_2$ (1:99); (b) 1 wt % Au/CuO$_x$−TiO$_2$ (2:98); (c) 1 wt % Au/CuO$_x$−TiO$_2$ (4.8:95.2); (d) 1 wt % Au/CuO$_x$−TiO$_2$ (10:90).

most particles still were less than 3 nm with hemispherical shape on the support.

3.4. XPS. The Cu 2p spectra of Au/CuO$_x$−TiO$_2$ catalysts with different Cu/Ti ratios are shown in Figure 5. The Cu 2p$_{3/2}$ and Cu 2p$_{1/2}$ spectra were centered at 933 and 953 eV, respectively. The Cu 2p$_{3/2}$ and Cu 2p$_{1/2}$ binding energy of the sample was slightly higher than the values of pure CuO reported by Chang et al.[24] The higher binding energy was possibly caused by the interaction between CuO$_x$ and TiO$_2$, resulting in the shift of the Cu binding energy.[10,25] It appears that almost 50% of Cu was in metallic state. By comparing the standard binding

Table 2. XPS Analysis for the Element State of Au and Cu

	Au species		Cu species		IAu4f/
	Au^{3+}	Au^0	Cu^{2+}	Cu^0	(ITi2p +
catalyst	(%)	(%)	(%)	(%)	ICu2p)
1% Au/CuO$_x$−TiO$_2$ (1:99)	17	83	65	35	0.049
1% Au/CuO$_x$−TiO$_2$ (2:98)	14	86	62	38	0.061
1% Au/CuO$_x$−TiO$_2$ (4.8:95.2)	7	93	51	49	0.056
1% Au/CuO$_x$−TiO$_2$ (10:90)	5	95	54	46	0.058
1% Au/CuO$_x$−TiO$_2$ (2:98), PROX	4.5	95.5	52	48	0.063

energy of Au at 84 and 88 eV in Figures 6 and 7, there is obviously a higher shift. The 1% Au/CuO$_x$−TiO$_2$ (1:99) showed around +1 eV shift, other catalysts showed about +2 eV shift. It indicates that there was an interaction between the Cu−Ti support and Au species. The Au 4f$_{7/2}$ and Au 4f$_{5/2}$ peaks were much closer than the others; the added amount of Cu could affect the elemental state of Au.

As shown in Table 2, the concentration of oxidic gold species decreased with the increasing Cu/Ti ratio. It is proposed[20] that both Au^0 and Au^{3+} were required for higher activity in PROX. Au^0 is considered to adsorb CO, while Au^{3+} cemented the metallic particle on the support and activate surface hydroxyl groups, which can react with the adsorbed CO to form adsorbed carboxylate. The highly dispersed gold particles (Au^0 and Au^{3+}) are responsible for the superior catalytic performance. The catalytic activity decreased with decreasing Au^{3+} content.

The surface composition of the catalyst was also investigated by XPS. For the surface element analysis, Au/(Cu + Ti) atomic ratio was about 0.0048−0.0052 for 1% Au/CuOx−TiO$_2$ catalysts, which is in agreement with the expected value for the bulk composition of the sample with 1 wt % Au content (Au/(Cu+Ti) = 0.0046). Moreover, the XPS peak intensity ratios of IAu4f/(ITi2p + ICu2p) were determined to identify the dispersion threshold of Au in CuO$_x$−TiO$_2$.[13] The IAu2p/(ITi2p + ICu2p) values were smaller than 0.07, indicating that Au was well-dispersed on the support.

3.5. Catalytic Activity. Figure 8a,b shows the effect of Cu/Ti molar ratios for the preferential oxidation of CO over Au/CuO$_x$−TiO$_2$ and Au/TiO$_2$ catalysts. Addition of suitable amount of CuO$_x$ improved the CO conversion. In the operating temperature for fuel cell (~80 °C), Au/CuOx−TiO$_2$ catalysts showed superior activity than Au/TiO$_2$. The activity of Au/TiO$_2$ increased with increasing temperature until it reached the maximum CO conversion of 97% at 65 °C. Then the activity decreased to 78% at 100 °C. It is well-known that although TiO$_2$ is an effective support for Au to selectively oxidize CO, the conversion will decrease appreciably. It is observed that there is no significant difference in the Cu/Ti ratios of 1/99, 2/98, and 4.8/95.2 in Au/CuO$_x$−TiO$_2$ catalysts when the temperature was above 35 °C. The CO conversions of these catalysts achieved ~99%, and the activity could be maintained at high temperature. Generally, the CO conversion slightly decreased with increasing CuO$_x$ content. Although Au/CuO$_x$−TiO$_2$(10:90) had a lower activity, the CO conversion could reach 95% at 80 °C. It indicates that CuO$_x$ promoted Au to be active at high temperature. CuO$_x$ played the role of a promoter but not as an active site. If CuO$_x$ is the active site as Au, the higher CuO$_x$ content should induce higher CO conversion. Therefore, CuO$_x$−TiO$_2$ was proposed to be a supplier or storage of oxygen. Suitable CuO$_x$ content formed new support properties to increase catalytic activity of CO oxidation.

CuO$_x$ can inhibit H$_2$ oxidizing to H$_2$O. Hence the CO selectivity increased upon addition of CuO$_x$. The selectivity of Au/TiO$_2$ decreased sharply, due to the nature of TiO$_2$. When the temperature was higher than 65 °C, the selectivity was less
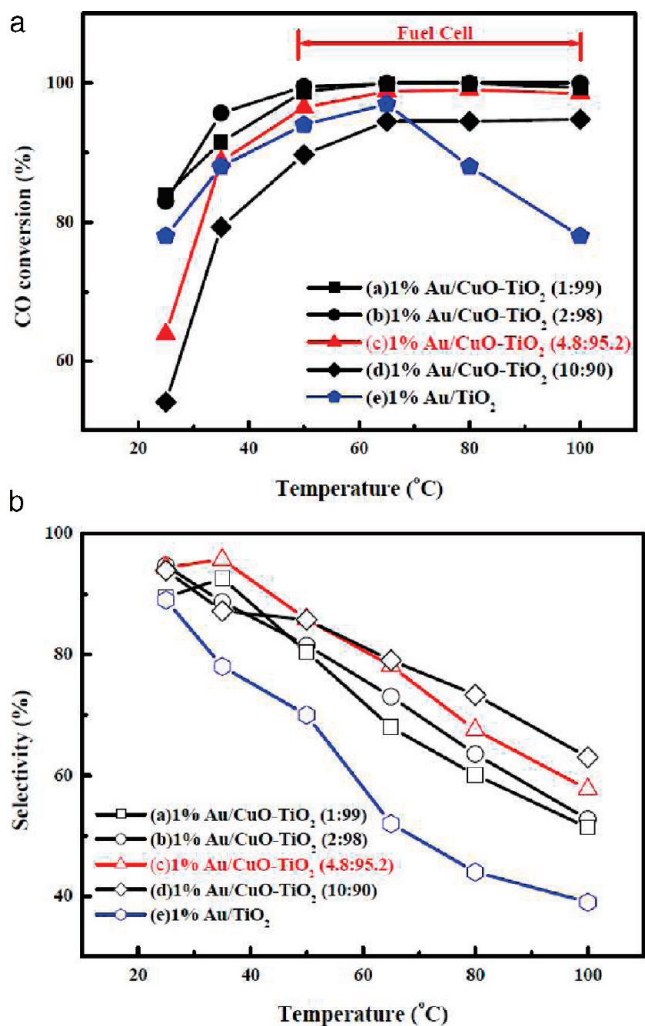

Figure 8. (Panel a) Effect of Cu/Ti mole ratios over Au/CuO$_x$−TiO$_2$ catalysts for CO conversion; (panel b) effect of Cu/Ti mole ratios over Au/CuO$_x$−TiO$_2$ catalysts for CO selectivity: (a) 1 wt % Au/CuO$_x$−TiO$_2$ (1:99); (b) 1 wt % Au/CuO$_x$−TiO$_2$ (2:98); (c) 1 wt % Au/CuO$_x$−TiO$_2$ (4.8:95.2); (d) 1 wt % Au/CuO$_x$−TiO$_2$ (10:90); (e) 1 wt % Au/TiO$_2$.
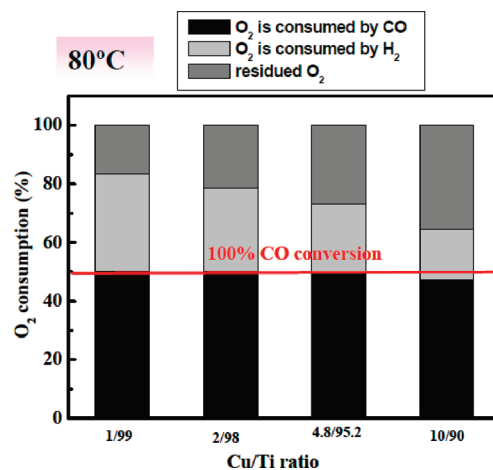

Figure 9. The condition of O$_2$ consumption at 80 °C.

than 50%. It indicates that H$_2$ competed with CO to capture oxygen. In thermodynamics, the exothermic enthalpy of H$_2$ reacting with oxygen is lower than that with CO. At high temperature, it is estimated that H$_2$ would keep CO from adsorbing on Au active site. In Figure 9, it shows that after
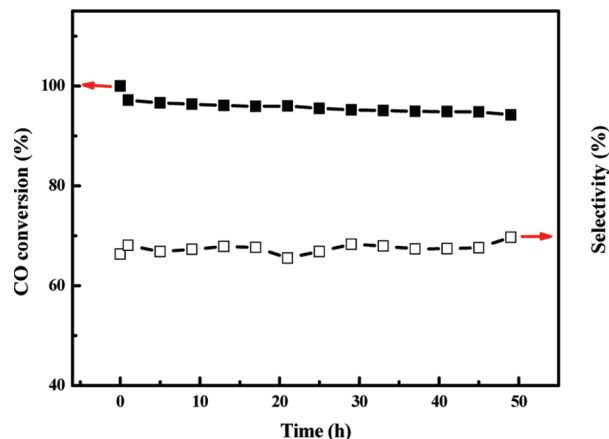
Figure 10. CO conversion and selectivity of 1% Au/CuO$_x$−TiO$_2$ (4.8:95.2) at 80 °C for 49 h time on stream.

adding CuO$_x$ on the support, CuO$_x$ modified the support and prevented the comparative H$_2$ oxidation. Au/CuO$_x$−TiO$_2$ catalysts with Cu/Ti ratios of 1/99, 2/98, and 4.8/95.2 had similar CO conversion; all reached 100% at 80 °C. Au/CuO$_x$−TiO$_2$ (4.8:95.2) had the highest selectivity of oxygen reacting with CO, which was about 60%. Au/CuO$_x$−TiO$_2$ catalysts show a potential application for the PROX reaction, which is used to remove trace amount of CO from hydrogen for fuel cell applications. The catalytic activity depends on the gold complex and particle size. Au/CuO$_x$−TiO$_2$ catalysts have similar particle size; the actual effect of CO conversion may be due to the state of gold and the support. One wt % Au/CuO$_x$−TiO$_2$ (4.8:95.2) is the most suitable catalyst for PROX with high CO conversion and high CO selectivity at fuel cell operation temperature. In long time test, 1 wt % Au/CuOx−TiO$_2$ (4.8:95.2) was tested at 80 °C for 49 h. In TEM images, the gold particle size was about 3 nm, implying that the catalysts were stable. To study the effect upon storage environment, the catalysts were stored in a dark box and downpour for one month. The CO conversion of the former became lower, and the latter was less active. It indicates that atmosphere indeed affects the catalytic performance. Even after storage for one month, the catalytic performance still remained in good condition as shown in Figure 10.

4. Conclusion

A series of Au/CuO$_x$−TiO$_2$ with various CuO$_x$ content were prepared. CuO$_x$−TiO$_2$ support was prepared by incipient-wetness impregnation. Au was load by deposition−precipitation method. The nominal Au content was 1 wt %. The real Au content on CuO$_x$−TiO$_2$ support was much greater than that on pure TiO$_2$. Au/CuO$_x$−TiO$_2$ with various Cu/Ti molar ratios showed similar gold particle size, which was about 2.3−2.5 nm. Au/CuO$_x$−TiO$_2$ catalysts calcined at 180 °C had a superior catalytic activity and selectivity for CO oxidation at reaction temperature of >80 °C. The catalytic activity of the catalysts was closely related to the state of gold in the catalysts. The highly dispersed and poorly crystallized metallic gold and small amount of oxidized gold in the catalysts exhibited superior catalytic activity for CO oxidation in PROX reaction.

For XPS analysis, Au^0 and Au^{3+} both played the active roles in PROX reaction. Au/CuO$_x$−TiO$_2$ had more metallic gold with increasing Cu/Ti ratio. Au/CuO$_x$−TiO$_2$ (4.8:95.2) had the best catalytic performance at high temperature. It contained 6% Au^{3+} and 94% Au^0. Catalysts consisting of more CuO$_x$ reduced the CO conversion but improved the CO selectivity. At fuel cell operating temperature (50−100 °C), the catalysts with Cu/Ti

of 1/99, 1/98, and 4.8/95.2 had similar CO conversion (∼100%). Moreover, considering the CO selectivity, Cu/Ti of 4.6/95.2 was the best ratio. Au/CuO$_x$−TiO$_2$ showed no obvious CuO$_x$ and Au diffraction peaks in XRD patterns, indicating that the particles were small and well dispersed. Au/CuO$_x$−TiO$_2$ (Cu/Ti = 4.8/95.2) had CO conversion of 100% at 80 °C and 68% CO selectivity. Gold particles were well dispersed and stable. Even after PROX reaction at 80 °C for 49 h, most of the particle still maintained at ∼2.4 nm. The CO conversion slightly decreased from 100% to 95%, and CO selectivity was nearly the same. Au/CuO$_x$−TiO$_2$ is a highly effective and thermally stable catalyst for PROX reaction.

Acknowledgment

Literature Cited

(1) Bond, G. C.; Thompson, D. T. Catalysis by gold. *Catal. Rev.-Sci. Eng.* **1999**, *41*, 319–388.

(2) Haruta, M. Size- and support-dependency in the catalysis of gold. *Catal. Today* **1997**, *36*, 153–166.

(3) Haruta, M.; Tsubota, S.; Kobayashi, T.; Kageyama, H.; Genet, M. J.; Delmon, B. Low-temperature oxidation of CO over gold-supported on TiO$_2$, α-Fe$_2$O$_3$, and Co$_3$O$_4$. *J. Catal.* **1993**, *144*, 175–192.

(4) Valden, M.; Lai, X.; Goodman, D. W. Onset of catalytic activity of gold clusters on titania with the appearance of nonmetallic properties. *Science* **1998**, *281*, 1647–1650.

(5) Haruta, M.; Yamada, N.; Kobayashi, T.; Iijima, S. Gold catalysts prepared by coprecipitation for low-temperature oxidation of hydrogen and of carbon monoxide. *J. Catal.* **1989**, *115*, 301–309.

(6) Moreau, F.; Bond, G. C.; Taylor, A. O. Gold on titania catalysts for the oxidation of carbon monoxide: Control of pH during preparation with various gold contents. *J. Catal.* **2005**, *231*, 105–114.

(7) Okumura, M.; Nakamura, S.; Tsubota, S.; Nakamura, T.; Azuma, M.; Haruta, M. Chemical vapor deposition of gold on Al$_2$O$_3$, SiO$_2$, and TiO$_2$ for the oxidation of CO and of H$_2$. *Catal. Lett.* **1998**, *51*, 53–58.

(8) Li, W. C.; Comotti, M.; Schuth, F. Highly reproducible syntheses of active Au/TiO$_2$ catalysts for CO oxidation by deposition−precipitation or impregnation. *J. Catal.* **2006**, *237*, 190–196.

(9) Bamweda, G. R.; Tsubota, S.; Nakamura, T.; Haruta, M. The influence of the preparation methods on the catalytic activity of platinum and gold supported on TiO$_2$ for CO oxidation. *Catal. Lett.* **1997**, *44*, 83–87.

(10) Friedman, R. M.; Freeman, J. J.; Lytle, F. W. Characterization of Cu/Al$_2$O$_3$ catalysts. *J. Catal.* **1978**, *55*, 10–28.

(11) Liu, W.; Flytzani-Stephanopoulos, M. Transition metal-promoted oxidation catalysis by fluorite oxides: A study of carbon monoxide oxidation over Cu−CeO$_2$. *Chem. Eng. J.* **1996**, *64*, 283–294.

(12) Yu, X. F.; Wu, N. Z.; Xie, Y. C.; Tang, Y. Q. A monolayer dispersion study of titania-supported copper oxide. *J. Mater. Chem.* **2000**, *10*, 1629–1634.

(13) Huang, J. S.; Wang, Y.; Zhao, X.; Wang, S.; Wu, S.; Huang, W. Synthesis and characterization of CuO/TiO$_2$ catalysts for low-temperature CO oxidation. *Catal. Commun.* **2006**, *7*, 1029–1034.

(14) Liu, Z. M.; Vannice, M. A. CO and O$_2$ adsorption on model Au−TiO$_2$ systems. *Catal. Lett.* **1997**, *43*, 51–54.

(15) Chang, L. H.; Sasirekha, N. R.; Chen, Y. W. Au/ MnO$_2$−TiO$_2$ catalyst for preferential oxidation of carbon monoxide in hydrogen stream. *Catal. Commun.* **2007**, *8*, 1702–1710.

(16) Chang, L. H.; Sasirekha, N. R.; Chen, Y. W. Preferential oxidation of carbon monoxide in hydrogen stream over Au/MgO$_x$−TiO$_2$ Catalysts. *Ind. Eng. Chem. Res.* **2008**, *47*, 4098–4105.

(17) Chang, L. H.; Sasirekha, N. R.; Chen, Y. W. CO oxidation on ceria and manganese oxide-supported gold catalysts. *Sep. Purif. Technol.* **2007**, *58*, 211–218.

(18) Chang, L. H.; Sasirekha, N. R.; Chen, Y. W.; Wang, W. J. Preferential oxidation of CO in H$_2$ stream over Au/MnO$_2$−CeO$_2$ catalysts. *Ind. Eng. Chem. Res.* **2006**, *45*, 4927–4935.

(19) Haruta, M. Nanoparticulate gold catalysts for low-temperature CO oxidation. *J. New Mater. Electrochem. Syst.* **2004**, *7*, 163–172.

(20) Boccuzzi, F.; Chiorino, A.; Manzoli, M.; Lu, P.; Akita, T.; Ichikawa, S.; Haruta, M. Au/TiO$_2$ nanosized samples: A catalytic, TEM, and FTIR

study of the effect of calcination temperature on the CO oxidation. *J. Catal.* **2001**, *202*, 256–267.

(21) Akita, T.; Lu, P.; Ichikawa, S.; Tanaka, K.; Haruta, M. Analytical TEM study on the dispersion of Au nanoparticles in Au/TiO₂ catalyst prepared under various temperatures. *Surf. Interface Anal.* **2001**, *31*, 73–78.

(22) Stangland, E. E.; Stavens, K. B.; Andres, R. P.; Delgass, W. N. Characterization of gold−titania catalysts via oxidation of propylene to propylene oxide. *J. Catal.* **2000**, *191*, 332–337.

(23) Bandara, J.; Udawatta, C. P. K.; Rajapakse, C. S. K. Highly stable CuO incorporated TiO₂ catalyst for photocatalytic hydrogen production from H₂O. *Photochem. Photobiol. Sci.* **2005**, *4*, 857–861.

(24) Chang, S. S.; Lee, H. J.; Park, H. J. Photoluminescence properties of spark-processed CuO. *Ceram. Int.* **2005**, *31*, 411–415.

(25) Strohmeier, B. R.; Leyden, D. E.; Field, R. S.; Hercules, D. M. Surface spectroscopic characterization of Cu/Al₂O₃ catalysts. *J. Catal.* **1985**, *94*, 514–530.